

Protective Effects of Nanosof[®] Suspension on Cultured Cells Exposed to H₂O₂

Antonia Teona Deftu^{1,2} , Bogdan Amuzescu^{1,2,*} 

¹ Department of Anatomy, Animal Physiology and Biophysics, Faculty of Biology, University of Bucharest, 91–95 Splaiul Independentei, Bucharest 050095, Romania; teona.deftu@yahoo.com (A.T.D.); bamuzesc@yahoo.com (B.A.); bogdan@biologie.kappa.ro (B.A.);

² Life, Environmental and Earth Sciences Division, Research Institute of the University of Bucharest (ICUB), 91–95 Splaiul Independentei, Bucharest 050095, Romania

* Correspondence: bogdan@biologie.kappa.ro (B.A.);

Scopus Author ID 55609161000

Received: 23.04.2021; Revised: 28.05.2021; Accepted: 3.06.2021; Published: 24.06.2021

Abstract: Nanoparticle and nanomaterial-based treatments have improved a lot recently in terms of bioavailability, effectiveness, and reduced toxic and side effects. Many studies found a protective effect of fullerene C₆₀ derivatives as potent free radical scavengers in biological systems and also showed neuroprotective properties when tested on *in vivo* models of ischemic stroke. This study assessed the antioxidant effects of Nanosof[®] powder suspension, an oxygenated fullerene compound, on various cell types exposed to exogenous free oxygen radicals. Cor.4U[®] cardiomyocytes and bEnd.3, BV-2, HEK293/hERG1 cell lines were treated with Nanosof[®] powder suspension alone or during exposure to 100 μM H₂O₂ for 24 h, in order to check the nanoparticle capacity to neutralize reactive oxygen species, using MTS or MTT to assess viability. We found no significant change in the viability of cells treated with Nanosof[®] compared to control. In the presence of H₂O₂, Nanosof[®] increased cell viability compared to H₂O₂ exposure alone. Nanosof[®] treatment showed no side effect; moreover, it exerted a protective effect on all three tested cell lines and Cor.4U[®] cardiomyocytes, indicating that treatment with this oxygenated fullerene may benefit various conditions.

Keywords: cardiomyocyte; endothelial cells; hydrogen peroxide; microglia; oxygenated fullerenes; viability assay.

© 2021 by the authors. This article is an open-access article distributed under the terms and conditions of the Creative Commons Attribution (CC BY) license (<https://creativecommons.org/licenses/by/4.0/>).

1. Introduction

The field of nanotechnology evolved steadily during the last decade, providing a variety of alternative approaches or complementary medications [1-5]. New nanotechnology achievements [6-9] have contributed to a better understanding of the complex etiopathogenesis of some widespread diseases, particularly in neurology [10-18]. Several metallic and organic nanomaterials have been approved by the US FDA (United States Food and Drug Administration) at different clinical trial stages as diagnostic tools [19].

Biocompatibilization by conjugation of fullerene-based molecules has become a primary strategy in overcoming the intrinsic obstacles encountered by fullerenes to utilize them for biological purposes. Consequently, assays aiming to apply fullerenes in different physicochemical and pharmacological research areas extend at an alert pace, and breakthroughs and developments frequently occur [20-24].

1.1. Neuroprotective effects of fullerene C₆₀ derivatives.

In order to improve the bioavailability and reduce the toxic and side effects, nanotechnology treatments have improved a lot in recent years. Neurodegenerative diseases are common among older people and a major social and medical problem. Receptors of blood-brain barrier (BBB) endothelial cells have been used as therapeutic targets for this kind of disease [25]. However, even though circulating fullerenes are in direct contact with vascular endothelial cells, few studies have addressed their effect on cerebral endothelial cells [26]. In particular, the capacity of fullerenes to modulate the BBB properties of brain-derived microvascular endothelial cells has not been investigated so far. Water-soluble polyhydroxylated fullerene derivatives known as fullerlenols or fullerols might counteract oxidative stress via the extracellular-signal-regulated kinase (ERK1/2) and nuclear factor- κ B (NF κ B) pathways, and thus can protect microvascular endothelial cells under inflammatory conditions [27].

Due to unique physicochemical properties, relative biocompatibility, and versatility in surface modification with various molecules, fullerene C₆₀ and its derivatives have been investigated as a novel way to improve modalities used to diagnose, monitor, and treat certain chronic diseases [28-30]. Due to their pharmacological properties, water-soluble fullerene derivatives are some of the compounds used to treat and prevent acute and chronic neurodegenerative disorders [31].

Previous studies have shown that activated microglia release neurotoxic factors that can cause toxicity to neurons. This indirect toxicity could also play important roles in developing neurodegenerative diseases, including prion diseases [32,33]. A study demonstrated that C₆₀(OH)_n (usually $n = 24$) inhibits cellular prion protein PrP(106-126)-induced excessive production of pro-inflammatory cytokines and toxic molecules in BV-2 rat microglial cells [31]. C₆₀(OH)_n does not exert cytotoxicity to BV-2 cells at a concentration less than 100 μ M, and a similar concentration range was used to evaluate biological activities of C₆₀(OH)_n *in vitro* [34-36]. In general, BBB restricts the entry of many potentially therapeutic agents into the brain. But there is evidence showing that water-soluble C₆₀ derivatives delivered by intraperitoneal injection or oral administration can cross BBB *in vivo*, showing significant benefits in neurological disorders. C₆₀(OH)_n are also effective in modulating the activation of microglial cells and reducing indirect toxicity *in vitro*. The increasing use of fullerene materials warrants toxicological investigations *in vivo*. C₆₀(OH)_n administered by intraperitoneal injection or oral administration might reduce inflammation and confer neuroprotection *in vivo* in a model of prion disease. The anti-inflammatory activity of fullerlenol C₆₀(OH)₂₄ was associated with activation of Nrf2/ARE (transcription factor NF-E2-related factor 2/antioxidant responsive element) pathway, providing insight into the underlying mechanism of neuroprotective effects of C₆₀ derivatives. Although more studies are needed to further explore and confirm initial findings, these results might help design and utilize fullerenes and their derivatives as therapeutic approaches for the treatment of prion disease and an attractive strategy to prevent neurodegenerative diseases associated with it inflammation [31].

Synthesis of water-soluble fullerene derivatives is thought to be a promising strategy to protect cells against apoptosis by attenuating oxidative stress [37]. A water-soluble C₆₀-GSH derivative was synthesized and its cell-protective effects were proved, including inhibition of intracellular reactive oxygen species (ROS) production, improved cell viability and remarkable alleviation of H₂O₂-induced cell apoptosis without evident toxicity in HEK293T cells [38].

1.2. Antiischemic effects of fullerene C₆₀ derivatives.

Many studies found protective effects of fullerene C₆₀ derivatives as potent free radical scavengers in biological systems [39]. Some studies confirmed that pretreatment with Frl (one of these nanoparticles) completely prevented heart rate variability (HRV) alterations induced by doxorubicin (an anti-cancer drug known to exert cardiotoxic side effects), decreased oxidative stress and normalized myocardial histopathological score, therefore it may play a role in the prevention of acute doxorubicin-induced cardiotoxicity [40-42]. Another remarkable effect is activation by C₆₀ of mitogen-activated protein kinase (MAPK) expression level resulting in improved brown adipose stem cells survival, proliferation and cardiomyogenic differentiation [43].

A single C₆₀ sphere can catch as many as 34 methyl radicals, leading to a description of this molecule as a „radical sponge” [44]. Free radical-scavenging properties have been confirmed by quantum-mechanical simulations [45]. Fullerene derivatives also cause the recovery of glutathione (GSH) [46] and nitric oxide (NO) [47], thus supporting free radicals removal. In addition, fullerene derivatives have shown neuroprotective properties *in vivo* models of ischemic stroke [48].

1.3. Characterization of Nanosof[®].

Nanosof[®] is an oxygenated fullerene chemically heterogeneous product (over 80% elemental oxygen content) obtained by original methods from carbon products of animal origin. The product was previously tested in multiple *in vitro*, *in vivo*, and clinical trials and was shown to exert several remarkable therapeutic effects, most notably an increased scavenging effect on free oxygen radicals and potentiating effects on the antioxidant properties of other antioxidants of natural origin. These properties are exploited in the commercially available product Nanoxyn alpha, a product approved by FDA as a food supplement and delivered on the US market (more data available on the company website <https://nanoxyn.ro/en/>).

1.4. Oxidative stress.

Oxidative stress, which can be induced by endogenous or exogenous free radicals such as H₂O₂, plays a crucial role in many acute and chronic diseases, including ischemia-reperfusion injury [49], viral infections [50], neurodegenerative diseases [51-53] and cancer [54], therefore a large variety of natural or artificial antioxidants have been tested as therapeutic agents [55-57]. Studies aiming to resolve this problem have been continued for decades, but the underlying mechanisms are still not fully understood. H₂O₂, a significant ROS resource, has been widely used to induce exogenous oxidative stress in many different cell models. Previous studies indicated that H₂O₂-induced oxidative stress and cell apoptosis were associated with ROS generation and intracellular calcium mobilization regulated by the Bcl-2 family and subsequent caspase cascade activation [58,59]. Indeed, free radicals scavengers and antioxidants have been used to attenuate H₂O₂-induced cell apoptosis, which has attracted considerable attention recently [38].

1.5. Objectives.

This study aims to assess the antioxidant effects of Nanosof[®] powder suspension, an oxygenated fullerene compound, on various cell types exposed to exogenous free oxygen radicals in order to certify new efficient treatments in various conditions, following *in vitro* <https://biointerfaceresearch.com/>

experiments. Different human or animal cell lines, including bEnd.3 (mouse endothelial cells), BV-2 (rat microglia) and HEK293T/hERG1 (human embryonic diploid), and Cor.4U[®] cardiomyocytes (human stem cell-derived), were treated with Nanosof[®] powder suspension alone or in the presence of hydrogen peroxide (H₂O₂) in order to check the nanoparticle scavenging capacity using MTS or MTT viability assays.

2. Materials and Methods

2.1. Study design.

This study was performed entirely *in vitro* on primary cultures or cell lines and did not include experiments on humans or animals. All experiments were performed in triplicate. The investigations were carried out following the rules of the Declaration of Helsinki of 1975 (<https://www.wma.net/what-we-do/medical-ethics/declaration-of-helsinki/>), revised in 2013, and were approved by the Ethics of Scientific Research Commission of the University of Bucharest (approval 115/11.11.2016).

After seeding the cells in 12 wells of a 96-well plate for each cell type in a total volume of 100µl/well, the plate was left overnight in the incubator at 37 °C. 3 wells were used for background read-outs and were filled with 100µl of medium each, devoid of cells.

		H ₂ O ₂ (-)			H ₂ O ₂ (100 µM)								
		1	2	3	4	5	6	7	8	9	10	11	12
Nanosof (-)	A												
Nanosof (+)	B												
Nanosof (-)	C	Bg	Bg	Bg									
	D												
	E												
	F												
	G												
	H												

Figure 1. Experimental cell culture pattern in 96-well plates for the MTS or MTT cell viability test.

During the following day, the medium of the 12 cell-seeded wells for each plate was discarded and replaced with medium supplemented with specific factors, according to the pattern specified in Figure 1. Thus, in each plate, 3 of the 12 cell-containing wells were treated for 24 hours with normal cell culture medium (no treatment added, or double-negative control); 3 wells were treated for 24 hours with 100 µM H₂O₂; 3 wells were treated for 24 hours with 100µM H₂O₂ with Nanosof[®] suspension; 3 wells were treated for 24 hours with Nanosof[®] suspension only; for the 3 wells used for background spectrophotometer read-outs, the medium was also replaced with fresh normal medium. Hydrogen peroxide (H₂O₂) treatment is a well-known and widely used method of exposure of biological systems to exogenous free oxygen radicals. Therefore cells exposed to 100 µM H₂O₂ (for 24 h) were used as a positive control, while those exposed only to Nanosof[®] suspension were used as a control for effects on cell viability of this compound *per se*.

After 24 hours of incubation in specific conditions at 37 °C, viability assays were performed.

2.2. Experimental procedures.

2.2.1. Preparation and cultivation of cells.

Cells from the Balb/c mouse cell line bEnd.3 (passage 10-20; #ATCCr CRL-2299tm, American Type Culture Collection, VA, USA) were maintained in DMEM (Gibco, 12491-015) supplemented with 10% fetal bovine serum (Gibco, 10270-098), 1% Penicillin/Streptomycin (Gibco 15140-122), 2 mM L-Glutamine (Gibco, 25030-081), and 250 µg/ml Amphotericin B (Gibco, 15290-026) in a 5% CO₂ atmosphere at 37°C, as described previously [60].

BV-2, a retrovirus-immortalized microglia cell line primarily obtained from the rat brain, was maintained in DMEM (10-013-CVR, Corning) + 10% fetal bovine serum (F7524, Gibco) + 1% Penicillin/Streptomycin (P4458, Sigma) in a 5% CO₂ atmosphere at 37°C.

HEK293T/hERG1 (human embryo kidney 293 cells stably transfected with the *human ether-à-go-go-related gene 1* K⁺ channel), a human diploid cell line extracted from the embryonic kidney (metanephros), expressing the main transmembrane subunit of the human cardiac ion channel hERG1 in combination with a neomycin/geneticin (G-418) resistance element, was maintained in DMEM (Sigma, D5523) supplemented with 1% Glutamax (Gibco, 35050), 0.5% Penicillin-Streptomycin (Sigma, P4458), 7.4 mM D(+)-Glucose (Merck, 1.08337.0250), 10% fetal bovine serum (Gibco, 10270-098), and 300 µg/ml G-418 (Sigma, A1720) in a humidified incubator at 5% CO₂ and 37°C.

Cor.4U[®] human stem cell-derived cardiomyocytes (Axiogenesis AG, Cologne, Germany, currently part of Ncardia) were thawed and cultured at high density on Geltrex[®]-precoated wells of 24-well plates in Cor.4U[®] medium according to manufacturer's instructions, in a 5% CO₂ atmosphere at 37 °C.

bEnd.3, BV-2 and HEK293T/hERG1 cell lines were detached from 25 cm² angled cell culture flasks (Nunc[®] Surface) following Trypsin-EDTA treatment (3 min at 37 °C) with sterile tips, centrifuged briefly (5 min at 1000 g), resuspended in control cell culture medium, and cell density was counted with a Bürker-Türk chamber and adjusted such as to plate 5000 cells per well in a 96-well cell culture plate with a flat bottom, up to a 100-µl final volume for each well. Each cell line was disposed of in 12 wells following a predefined pattern (Figure 1). The cells were grown overnight in a humidified incubator (37 °C, 5% CO₂). The same procedure was applied for Cor.4U[®] cardiomyocytes according to manufacturer's instructions.

2.2.2. Solutions and chemicals.

The Nanosof[®] powder was a kind gift from Nanotech Health SRL (Ilfov, Romania). Preparation of the Nanosof[®] powder suspension used for these experiments was performed according to manufacturer's instructions, mixing 1 mg of pure powder (with rusty red color and paramagnetic properties) per 1 ml of cell culture medium in a plastic tube, followed by moderate centrifuging (1 min at 3200 rpm into an Eppendorf microcentrifuge). The pellet was discarded, while the supernatant was collected with a sterile syringe and subsequently filtered through 0.22 µm filters (Millipore Millex[®] GP Filter units with Millipore Express[®] PES membranes). Before centrifuging, the Nanosof[®] primary suspension was vortexed.

2.2.3. Nanosof[®] administration.

The cells were cultured at a proper density of 5000 cells/well in 96-wells plates. The cultures were maintained for 24h at 5% CO₂ atmosphere at 37°C. The next day the cells were

treated with sterile-filtered Nanosof[®] suspension in culture medium following the manufacturer's instructions and/or with 100 μ M H₂O₂ for 24h. The following day the medium was removed and replaced with MTT or MTS, used for cell viability assay.

2.2.4. MTT assay for cell viability.

For assessment of the number of viable cells in treated and control groups, MTT (methylthiazolyldiphenyl-tetrazolium bromide) assay was performed after Nanosof[®] treatment. An MTT assay is a qualitative index of cell viability. Mitochondrial and cytosolic dehydrogenases of living cells reduce the yellow tetrazolium salt (MTT) to produce a purple formazan dye that can be detected spectrophotometrically [61].

The viability of the cells was determined by performing an MTT assay 24 h after treatment. The cells were seeded at a density of 5000 cells/well on 96-well plates in 100 μ L of medium and incubated at 37 °C for 24 h. Afterward, the medium was replaced with sterile-filtered Nanosof[®] suspension in medium and/or hydrogen peroxide in the medium at 100 μ l/well total volume, and the cells were incubated overnight at 37 °C. The next day the medium was replaced with 100 μ l/well culturing medium (serum-free) and MTT (Sigma, M2128) reduction was initiated by adding MTT to a final concentration of 1 mg/ml per well. After 3-4 h of incubation at room temperature, the reaction was stopped by removing the MTT-containing medium and adding 100-150 μ l of DMSO (Dimethyl Sulfoxide) to each well to dissolve the formazan crystals. The plate was shaken for 20 min and the amount of cellular MTT formazan product was determined by measuring absorbance using a FlexStation 3 microplate reader (Molecular Devices, San Jose, CA) at a test wavelength of 570 nm and a reference wavelength of 650 nm.

For normalization, the absorbance readings were divided by the adjusted averaged absorbance reading of untreated cells in control wells (double-negative control, not exposed to H₂O₂ or Nanosof[®] suspension) to obtain the proportion of cell viability. Background absorbance was corrected using triplicate sets of wells containing medium only (no cells) and MTT reagent as per the experimental well.

2.2.5. MTS assay for cell viability.

MTS [3-(4,5-dimethylthiazol-2-yl)-5-(3-carboxymethoxyphenyl)-2-(4-sulfophenyl)-2H-tetrazolium, inner salt] assay represents an *in vitro* cell viability test based on an organic tetrazolium compound and a coupling reagent via electron transfer [phenazine ethosulfate; PES], featuring high stability, and thus being able to combine with MTS to form a stable solution. Spectrophotometric absorbance at 490 nm, measured at 1-4 hours following application in a well, is proportional to the number of viable cells. Cells were seeded at 5000 cells/well in 96-well plates and left to attach overnight at 37 °C. After 24 h the cells were treated with sterile-filtered Nanosof[®] suspension (1 mg/ml) and/or hydrogen peroxide (100 μ M) overnight at 37 °C.

20 μ l of MTS solution were added to each well, and the plate was left at room temperature, in sterile conditions. Absorbance at 490 nm (for optical density - OD) and at 650 nm (for background) was read with the plate spectrophotometer at 1 h, 2 h, and 4 h since MTS addition. After 3 hours, the content of each well was mixed by gentle aspiration and release with a laboratory pipette 5-fold.

Reduction in cell viability relative to untreated cells was measured 24 h after the exposure, by MTS assay, following the manufacturer's protocol. The absorbance of each well was measured with a FlexStation 3 microplate reader (Molecular Devices) at 490 nm and at 650 nm for background. The proportion of viable cells in each well was normalized by division to the average of control wells. Triplicate sets of wells without cells incubated with MTS solution were used for background subtraction. All treatments are summarized in Table 1.

2.2.6. Statistical analysis.

All data measured by the microplate reader (FlexStation 3, Molecular Devices) were transferred and processed in Microsoft Excel. Statistical analysis of data was performed using a *two-tailed unpaired Student's t-test* and applied to evidence statistically significant differences between groups. Graphs in Figure 2 represent statistical significance as moderate * ($p < 0.05$), high ** ($p < 0.01$), and very high *** ($p < 0.001$). For $p > 0.05$, the tests were considered non-significant (ns). All data are reported as means \pm SEM and are normalized relative to averaged control values ($\text{H}_2\text{O}_2(-)\text{N}(-)$).

3. Results and Discussion

3.1. The effect of Nanosof[®] on bEnd.3 cells viability using MTS assay.

The MTS test showed that in the presence of H_2O_2 , Nanosof[®] increased bEnd.3 cell viability (relative viability 1.215 ± 0.069 , $n = 3$, $p < 0.01$) compared to H_2O_2 exposure alone (relative viability 0.554 ± 0.074 , $n = 3$). Compared to control (1 ± 0.015 , $n = 3$), the presence of Nanosof[®] alone increased cell viability (1.138 ± 0.025 , $n = 3$, $p < 0.01$) (Figure 2A).

3.2. The effect of Nanosof[®] on BV-2 cells viability using MTS assay.

In the presence of H_2O_2 , the MTS test showed that Nanosof[®] powder suspension increased BV-2 cell viability (relative viability 0.87 ± 0.087 , $n = 3$, $p < 0.05$) compared to H_2O_2 exposure alone (relative viability 0.507 ± 0.099 , $n = 3$). Nanosof[®] treatment showed no side effect ($p > 0.05$ for $\text{H}_2\text{O}_2(-)\text{N}(-)$ vs. $\text{H}_2\text{O}_2(-)\text{N}(+)$); moreover, it exerted a protective effect against oxidative stress ($p > 0.05$ for $\text{H}_2\text{O}_2(+)\text{N}(+)$ vs. $\text{H}_2\text{O}_2(-)\text{N}(-)$) (Figure 2B).

3.3. The effect of Nanosof[®] on HEK293T/hERG1 cells viability using MTS assay.

The MTS assay showed that in the presence of H_2O_2 , Nanosof[®] powder suspension increased HEK293/hERG cell viability (relative viability 0.506 ± 0.094 , $n = 3$, $p < 0.05$) compared to H_2O_2 exposure alone (relative viability 0.058 ± 0.051 , $n = 3$). Nanosof[®] treatment showed no side effect ($p > 0.05$ for $\text{H}_2\text{O}_2(-)\text{N}(-)$ vs. $\text{H}_2\text{O}_2(-)\text{N}(+)$). Compared to control (1 ± 0.062 , $n = 3$), the presence of Nanosof[®] powder suspension alone maintained good cell viability (relative viability 0.875 ± 0.069 , $n = 3$, $p > 0.05$) (Figure 2C).

3.4. The effect of Nanosof[®] on Cor.4U[®] cardiomyocytes cells viability using MTT assay.

In the presence of H_2O_2 , Nanosof[®] powder suspension increased cell viability (relative viability 0.789 ± 0.042 , $n = 3$, $p < 0.05$) compared to H_2O_2 exposure alone (relative viability 0.491 ± 0.096 , $n = 3$), using MTT viability assay. However, compared to control (1 ± 0.093 , $n = 3$), the presence of Nanosof[®] alone did not affect cell viability (0.93 ± 0.04 , $p > 0.05$ for $\text{H}_2\text{O}_2(-)\text{N}(-)$ vs. $\text{H}_2\text{O}_2(-)\text{N}(+)$) (Figure 2D).

Our results for all four cell culture preparations tested in this experiment indicate that Nanosof® suspension effectively neutralized the toxic effect on cell viability of hydrogen peroxide without being toxic for the cells *per se*. Figure 2 (A, B and C) illustrates MTS normalized cell viability values (mean of 3 wells for each tested condition). Figure 2D illustrates MTT normalized cell viability values (mean of 3 wells for each tested condition) at 4 h, following the dissolution of the formazan salt in DMSO. All absolute absorbance values are listed in Table 1.

Table 1. Cell viability test: absolute absorbance measured by the microplate reader for the 4 cell preparations tested.

Cell type	H ₂ O ₂ (-)N(-)			H ₂ O ₂ (+)N(-)			H ₂ O ₂ (-)N(+)			H ₂ O ₂ (+)N(+)			Test used
	Mean	SEM	n	Mean	SEM	n	Mean	SEM	n	Mean	SEM	n	
bEnd.3	0.65	0.0098	3	0.36	0.048	3	0.74	0.016	3	0.79	0.045	3	MTS
BV-2	0.69	0.0098	3	0.35	0.068	3	0.71	0.015	3	0.6	0.06	3	
HEK293	0.16	0.0099	3	0.0093	0.0081	3	0.14	0.011	3	0.081	0.015	3	
Cor.4U®	0.57	0.053	3	0.28	0.055	3	0.53	0.023	3	0.45	0.024	3	

H₂O₂(+) - cells exposed to H₂O₂ 100 μM for 24 h

H₂O₂(-) - cells non-exposed to H₂O₂

N(+) - cells exposed to Nanosof® powder suspension in medium

N(-) - cells non-exposed to Nanosof®

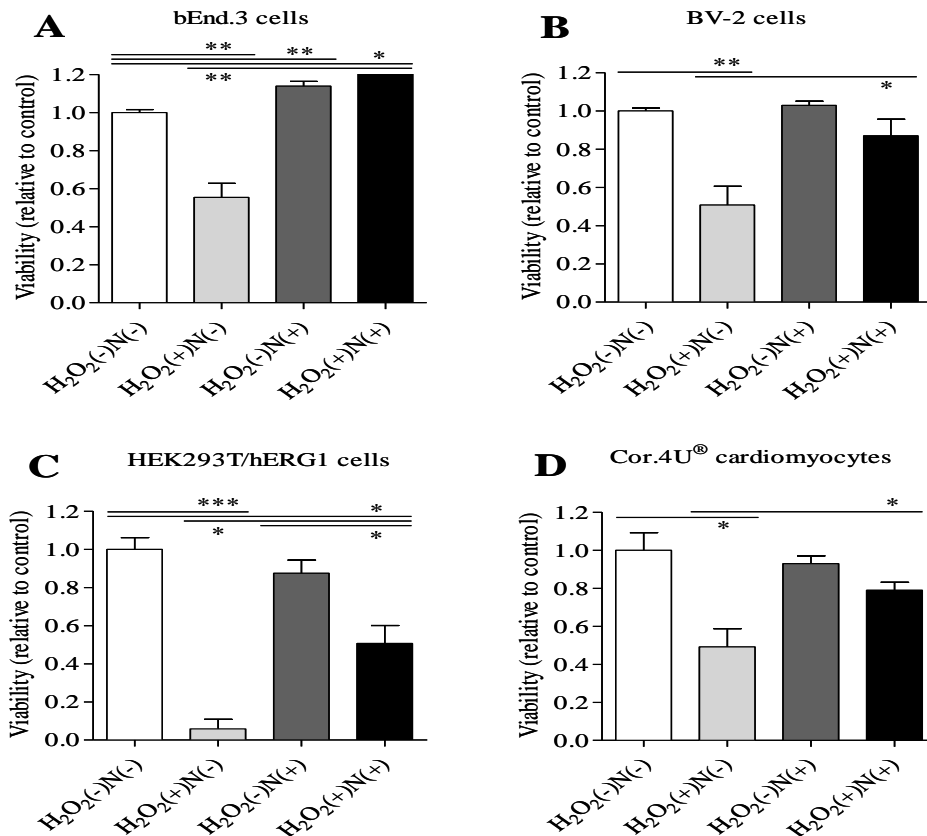


Figure 2. Effect of Nanosof® suspension on background cell viability and exposure to H₂O₂ for all four tested cell preparations. A. Effect of Nanosof® suspension on bEnd.3 cell viability; B. Effect of Nanosof® suspension on BV-2 cell viability; C. Effect of Nanosof® suspension on HEK293/hERG1 cell viability; D. Effect of Nanosof® suspension on Cor.4U® cardiomyocytes cell viability. For A, B and C, the values of absorbance at 490 nm following 4 h of exposure to MTS (mean for three wells/experimental condition) are shown; For D the values of absorbance at 570 nm following 4 h exposure to MTT, shortly after replacement with DMSO, are shown. Statistical significance is marked with * for $p < 0.05$, ** for $p < 0.01$, and *** for $p < 0.001$. Error bars represent the standard error of the means (SEM).

Our research provides direct experimental proofs for the free oxygen radicals scavenging capacity of Nanosof® powder suspension, which remarkably ameliorates H₂O₂-

induced cell apoptosis without evident toxicity in all tested cell preparations, confirming previous results with fullerenes and fullerenols applied *in vitro* to hydrogen peroxide-exposed cells [34,36,38] or to *in vivo* ischemia-reperfusion models [27,46,48].

Our results showed no significant change in the viability of cells treated with Nanosof[®] powder suspension compared to control. In the presence of H₂O₂, Nanosof[®] increased cell viability compared to H₂O₂ exposure alone. Nanosof[®] treatment showed no side effect; moreover, it exerted a protective effect on all three tested cell lines and Cor.4U[®] cardiomyocytes, indicating that treatment with this oxygenated fullerene may be beneficial in various conditions.

Nanosof[®] suspension applied in the presence of H₂O₂ exerted beneficial effects, possibly via scavenging or otherwise neutralizing exogenous free oxygen radicals, in all four tested cell preparations. Nanosof[®] suspension was not toxic and did not significantly influence cell viability for all three tested cell lines.

The exogenous free radical exposure model chosen for this experiment was adequate, resulting in significant decreases in cell viability for all four tested cell systems.

4. Conclusions

Nanosof[®] suspension could be useful in cell culture experiments for enhancing cell viability and limiting the deleterious effects of free radicals. For example, it could be used in the cell culture medium of human-induced pluripotent stem cell-derived cardiomyocytes to limit the toxic effects of free oxygen radicals on various cellular components, for example, on L-type calcium channels. We will seek to perform further tests concerning the effects of Nanosof[®] suspension on biological properties such as cell migration capacity. Nanosof[®] may be a new antioxidant treatment with broad clinical applicability.

Funding

This study was funded from Competitiveness Operational Programme 2014–2020 project P_37_675 (contract no. 146/2016), Priority Axis 1, Action 1.1.4, co-financed by the European Funds for Regional Development and Romanian Government funds.

Acknowledgments

The authors gratefully acknowledge Cornelia Dragomir and Geanina Haralambie for their support.

Conflicts of Interest

The authors have no actual or potential conflict of interest associated with this work.

References

1. Du, J.; Zhang, Y.S.; Hobson, D.; Hydbring, P. Nanoparticles for immune system targeting. *Drug Discov Today* **2017**, *22*, 1295-1301, <https://doi.org/10.1016/j.drudis.2017.03.013>.
2. Hejmady, S.; Pradhan, R.; Alexander, A.; Agrawal, M.; Singhvi, G.; Gorain, B.; Tiwari, S.; Kesharwani, P.; Dubey, S.K. Recent advances in targeted nanomedicine as promising antitumor therapeutics. *Drug Discov Today* **2020**, *25*, 2227-2244, <https://doi.org/10.1016/j.drudis.2020.09.031>.
3. Jin, G.; Zhao, X.; Xu, F. Therapeutic nanomaterials for cancer therapy and tissue regeneration. *Drug Discov Today* **2017**, *22*, 1285-7, <https://doi.org/10.1016/j.drudis.2017.08.002>.

4. Teleanu, D.M.; Chircov, C.; Grumezescu, A.M.; Teleanu, R.I. Neuronanomedicine: An Up-to-Date Overview. *Pharmaceutics* **2019**, *11*, 101, <https://doi.org/10.3390/pharmaceutics11030101>.
5. Wu, J.; Xie, L.; Lin, W.Z.Y.; Chen, Q. Biomimetic nanofibrous scaffolds for neural tissue engineering and drug development. *Drug Discov Today* **2017**, *22*, 1375-1384, <https://doi.org/10.1016/j.drudis.2017.03.007>.
6. Du, Y.; Alifu, N.; Wu, Z.; Chen, R.; Wang, X.; Ji, G.; Li, Q.; Qian, J.; Xu, B.; Song, D. Encapsulation-Dependent Enhanced Emission of Near-Infrared Nanoparticles Using in vivo Three-Photon Fluorescence Imaging. *Front Bioeng Biotechnol* **2020**, *8*, 1029, <https://doi.org/10.3389/fbioe.2020.01029>.
7. Liu, M.H.; Zhang, Z.; Yang, Y.C.; Chan, Y.H. Polymethine-Based Semiconducting Polymer Dots with Narrow-Band Emission and Absorption/Emission Maxima at NIR-II for Bioimaging. *Angew Chem Int Ed Engl* **2021**, *60*, 983-989, <https://doi.org/10.1002/anie.202011914>.
8. Radu, B.M.; Radu, M. Recent Preclinical and Clinical Technological Advances Suitable to Unravel the Physiological and Pathological Status of the Blood Brain Barrier in Neurology. *EC Neurology* **2015**, *1*, 22-28.
9. Xie, W.; Gong, X.T.; Cheng, X.; Cao, J.; Zhao, J.; Zhang, H.L.; Zhang, S. LIMPID: a versatile method for visualization of brain vascular networks. *Biomater Sci* **2021**, *9*, 2658-2669, <https://doi.org/10.1039/d0bm01817a>.
10. Asefy, Z.; Hoseinnejad, S.; Ceferov, Z. Nanoparticles approaches in neurodegenerative diseases diagnosis and treatment. *Neurol Sci* **2021**, *2021*, <https://doi.org/10.1007/s10072-021-05234-x>.
11. Brighi, C.; Reid, L.; Genovesi, L.A.; Kojic, M.; Millar, A.; Bruce, Z.; White, A.L.; Day, B.W.; Rose, S.; Whittaker, A.K.; Puttick, S. Comparative study of preclinical mouse models of high-grade glioma for nanomedicine research: the importance of reproducing blood-brain barrier heterogeneity. *Theranostics* **2020**, *10*, 6361-6371, <https://doi.org/10.7150/thno.46468>.
12. Dyne, E.; Prakash, P.S.; Li, J.; Yu, B.; Schmidt, T.L.; Huang, S.; Kim, M.H. Mild magnetic nanoparticle hyperthermia promotes the disaggregation and microglia-mediated clearance of Beta-amyloid plaques. *Nanomedicine* **2021**, *2021*, 102397, <https://doi.org/10.1016/j.nano.2021.102397>.
13. Fabene, P.F.; Navarro Mora, G.; Martinello, M.; Rossi, B.; Merigo, F.; Ottoboni, L.; Bach, S.; Angiari, S.; Benati, D.; Chakir, A.; Zanetti, L.; Schio, F.; Osculati, A.; Marzola, P.; Nicolato, E.; Homeister, J.W.; Xia, L.; Lowe, J.B.; McEver, R.P.; Osculati, F.; Sbarbati, A.; Butcher, E.C.; Constantin, G. A role for leukocyte-endothelial adhesion mechanisms in epilepsy. *Nat Med*. **2008**, *14*, 1377-83, <https://doi.org/10.1038/nm.1878>.
14. Gopalan, D.; Pandey, A.; Alex, A.T.; Kalthur, G.; Pandey, S.; Udupa, N.; Mutalik, S. Nanoconstructs as a versatile tool for detection and diagnosis of Alzheimer biomarkers. *Nanotechnology* **2021**, *32*, 1361-6528, <https://doi.org/10.1088/1361-6528/abcdeb>.
15. Liu, Y.; Liu, J.; Chen, D.; Wang, X.; Zhang, Z.; Yang, Y.; Jiang, L.; Qi, W.; Ye, Z.; He, S.; Liu, Q.; Xi, L.; Zou, Y.; Wu, C. Fluorination Enhances NIR-II Fluorescence of Polymer Dots for Quantitative Brain Tumor Imaging. *Angew Chem Int Ed Engl* **2020**, *59*, 21049-21057, <https://doi.org/10.1002/anie.202007886>.
16. Saavedra-Leos, M.Z.; Jordan-Alejandre, E.; López-Camarillo, C.; Pozos-Guillen, A.; Leyva-Porras, C.; Silva-Cázares, M.B. Nanomaterial Complexes Enriched With Natural Compounds Used in Cancer Therapies: A Perspective for Clinical Application. *Front Oncol* **2021**, *11*, 664380, <https://doi.org/10.3389/fonc.2021.664380>.
17. Salama, A.H.; A, A.A.S.; Elhabak, M. Single step nanospray drying preparation technique of gabapentin-loaded nanoparticles-mediated brain delivery for effective treatment of PTZ-induced seizures. *Int J Pharm* **2021**, *2021*, 120604, <https://doi.org/10.1016/j.ijpharm.2021.120604>.
18. Sarathlal, K.C.; Kakoty, V.; Krishna, K.V.; Dubey, S.K.; Chitkara, D.; Taliyan, R. Neuroprotective Efficacy of Co-Encapsulated Rosiglitazone and Vorinostat Nanoparticle on Streptozotocin Induced Mice Model of Alzheimer Disease. *ACS Chem Neurosci* **2021**, *2021*, <https://doi.org/10.1021/acscchemneuro.1c00022>.
19. Radu, B.M.; Radu, M.; Tognoli, C.; Benati, D.; Merigo, F.; Assalg, M.; Solani, E.; Stranieri, C.; Ceccon, A.; Fratta Pasini, A.M.; Cominacini, L.; Bramanti, P.; Osculati, F.; Bertini, G.; Fabene, P.F. Are they in or out? The elusive interaction between Qtracker [®] 800 vascular labels and brain endothelial cells. *Nanomedicine* **2015**, *10*, 3329-42, <https://doi.org/10.2217/nnm.15.120>.
20. Bartkowski, M.; Giordani, S. Supramolecular chemistry of carbon nano-onions. *Nanoscale* **2020**, *12*, 9352-9358, <https://doi.org/10.1039/d0nr01713b>.
21. Dong, R.; Liu, M.; Huang, X.X.; Liu, Z.; Jiang, D.Y.; Xiao, H.J.; Geng, J.; Ren, Y.H.; Dai, H.P. Water-Soluble C(60) Protects Against Bleomycin-Induced Pulmonary Fibrosis in Mice. *Int J Nanomedicine* **2020**, *15*, 2269-2276, <https://doi.org/10.2147/IJN.S214056>.
22. Kuo, W.S.; Chang, C.Y.; Liu, J.C.; Chen, J.H.; So, E.C.; Wu, P.C. Two-Photon Photoexcited Photodynamic Therapy with Water-Soluble Fullerenol Serving as the Highly Effective Two-Photon Photosensitizer Against Multidrug-Resistant Bacteria. *Int J Nanomedicine* **2020**, *15*, 6813-6825, <https://doi.org/10.2147/IJN.S236897>.
23. Maleki, R.; Khoshoei, A.; Ghasemy, E.; Rashidi, A. Molecular insight into the smart functionalized TMC-Fullerene nanocarrier in the pH-responsive adsorption and release of anti-cancer drugs. *J Mol Graph Model* **2020**, *100*, 107660, <https://doi.org/10.1016/j.jmgm.2020.107660>.
24. Yang, X.; Ebrahimi, A.; Li, J.; Cui, Q. Fullerene-biomolecule conjugates and their biomedical applications. *Int J Nanomedicine* **2014**, *9*, 77-92, <https://doi.org/10.2147/IJN.S52829>.

25. Duan, L.; Li, M.; Wang, C.; Wang, Q.; Liu, Q.; Shang, W.; Shen, Y.; Lin, Z.; Sun, T.; Quan, D.; Wu, Z. Study on synthesis and properties of nanoparticles loaded with amaryllidaceous alkaloids. *Open Life Sci* **2017**, *12*, 356-364, <https://doi.org/10.1515/biol-2017-0041>.
26. Gelderman, M.P.; Simakova, O.; Clogston, J.D.; Patri, A.K.; Siddiqui, S.F.; Vostal, A.C.; Simak, J. Adverse effects of fullerenes on endothelial cells: fulleranol C60(OH)24 induced tissue factor and ICAM-I membrane expression and apoptosis in vitro. *Int J Nanomedicine* **2008**, *3*, 59-68, <https://doi.org/10.2147/ijn.s1680>.
27. Schuhmann, M.K.; Fluri, F. Effects of Fullerenols on Mouse Brain Microvascular Endothelial Cells. *Int J Mol Sci* **2017**, *18*, 1783, <https://doi.org/10.3390/ijms18081783>.
28. Lin, C.M.; Lu, T.Y. C60 fullerene derivatized nanoparticles and their application to therapeutics. *Recent Pat Nanotechnol* **2012**, *6*, 105-13, <https://doi.org/10.2174/187221012800270135>.
29. Markovic, Z.; Trajkovic, V. Biomedical potential of the reactive oxygen species generation and quenching by fullerenes (C60). *Biomaterials* **2008**, *29*, 3561-73, <https://doi.org/10.1016/j.biomaterials.2008.05.005>.
30. Montellano, A.; Da Ros, T.; Bianco, A.; Prato, M. Fullerene C60 as a multifunctional system for drug and gene delivery. *Nanoscale* **2011**, *3*, 4035-41, <https://doi.org/10.1039/c1nr10783f>.
31. Ye, S.; Zhou, T.; Pan, D.; Lai, Y.; Yang, P.; Chen, M.; Wang, Y.; Hou, Z.; Ren, L.; Jiang, Y. Fullerene C60 Derivatives Attenuated Microglia-Mediated Prion Peptide Neurotoxicity. *J Biomed Nanotechnol* **2016**, *12*, 1820-33, <https://doi.org/10.1166/jbn.2016.2281>.
32. Caleo, M.; Restani, L.; Vannini, E.; Siskova, Z.; Al-Malki, H.; Morgan, R.; O'Connor, V.; Perry, V.H. The role of activity in synaptic degeneration in a protein misfolding disease, prion disease. *PLoS One* **2012**, *7*, e41182, <https://doi.org/10.1371/journal.pone.0041182>.
33. Hafner-Bratkovič, I.; Benčina, M.; Fitzgerald, K.A.; Golenbock, D.; Jerala, R. NLRP3 inflammasome activation in macrophage cell lines by prion protein fibrils as the source of IL-1 β and neuronal toxicity. *Cell Mol Life Sci* **2012**, *69*, 4215-28, <https://doi.org/10.1007/s00018-012-1140-0>.
34. Lao, F.; Chen, L.; Li, W.; Ge, C.; Qu, Y.; Sun, Q.; Zhao, Y.; Han, D.; Chen, C. Fullerene nanoparticles selectively enter oxidation-damaged cerebral microvessel endothelial cells and inhibit JNK-related apoptosis. *ACS Nano* **2009**, *3*, 3358-68, <https://doi.org/10.1021/nn900912n>.
35. Lao, F.; Li, W.; Han, D.; Qu, Y.; Liu, Y.; Zhao, Y.; Chen, C. Fullerene derivatives protect endothelial cells against NO-induced damage. *Nanotechnology* **2009**, *20*, 225103, <https://doi.org/10.1088/0957-4484/20/22/225103>.
36. Ye, S.; Chen, M.; Jiang, Y.; Chen, M.; Zhou, T.; Wang, Y.; Hou, Z.; Ren, L. Polyhydroxylated fullerene attenuates oxidative stress-induced apoptosis via a fortifying Nrf2-regulated cellular antioxidant defence system. *Int J Nanomedicine* **2014**, *9*, 2073-87, <https://doi.org/10.2147/IJN.S56973>.
37. Ritter, U.; Prylutskyy, Y.I.; Evstigneev, M.P.; Davidenko, N.A.; Cherepanov, V.V.; Senenko, A.I.; Marchenko, O.A.; Naumovets, A.G. Structural Features of Highly Stable Reproducible C60 Fullerene Aqueous Colloid Solution Probed by Various Techniques. *Fullerenes, Nanotubes and Carbon Nanostructures* **2015**, *23*, 530-4, <https://doi.org/10.1080/1536383X.2013.870900>.
38. Huang, J.; Zhou, C.; He, J.; Hu, Z.; Guan, W.C.; Liu, S.H. Protective effect of reduced glutathione C60 derivative against hydrogen peroxide-induced apoptosis in HEK 293T cells. *J Huazhong Univ Sci Technolog Med Sci* **2016**, *36*, 356-363, <https://doi.org/10.1007/s11596-016-1591-x>.
39. Shoji, M.; Takahashi, E.; Hatakeyama, D.; Iwai, Y.; Morita, Y.; Shirayama, R.; Echigo, N.; Kido, H.; Nakamura, S.; Mashino, T.; Okutani, T.; Kuzuhara, T. Anti-influenza activity of c60 fullerene derivatives. *PLoS One* **2013**, *8*, e66337, <https://doi.org/10.1371/journal.pone.0066337>.
40. Injac, R.; Perše, M.; Cerne, M.; Potočnik, N.; Radic, N.; Govedarica, B.; Djordjevic, A.; Cerar, A.; Strukelj, B. Protective effects of fulleranol C60(OH)24 against doxorubicin-induced cardiotoxicity and hepatotoxicity in rats with colorectal cancer. *Biomaterials* **2009**, *30*, 1184-96, <https://doi.org/10.1016/j.biomaterials.2008.10.060>.
41. Potočnik, N.; Perše, M.; Cerar, A.; Injac, R.; Finderle, Ž. Cardiac autonomic modulation induced by doxorubicin in a rodent model of colorectal cancer and the influence of fulleranol pretreatment. *PLoS One* **2017**, *12*, e0181632, <https://doi.org/10.1371/journal.pone.0181632>.
42. Torres, V.M.; Srdjenovic, B.; Jacevic, V.; Simic, V.D.; Djordjevic, A.; Simplício, A.L. Fulleranol C60(OH)24 prevents doxorubicin-induced acute cardiotoxicity in rats. *Pharmacol Rep* **2010**, *62*, 707-18, [https://doi.org/10.1016/s1734-1140\(10\)70328-5](https://doi.org/10.1016/s1734-1140(10)70328-5).
43. Hao, T.; Zhou, J.; Lü, S.; Yang, B.; Wang, Y.; Fang, W.; Jiang, X.; Lin, Q.; Li, J.; Wang, C. Fullerene mediates proliferation and cardiomyogenic differentiation of adipose-derived stem cells via modulation of MAPK pathway and cardiac protein expression. *Int J Nanomedicine* **2016**, *11*, 269-83, <https://doi.org/10.2147/IJN.S95863>.
44. Krusic, P.J.; Wasserman, E.; Keizer, P.N.; Morton, J.R.; Preston, K.F. Radical reactions of c60. *Science* **1991**, *254*, 1183-5, <https://doi.org/10.1126/science.254.5035.1183>.
45. Chistyakov, V.A.; Smirnova, Y.O.; Prazdnova, E.V.; Soldatov, A.V. Possible mechanisms of fullerene C₆₀ antioxidant action. *Biomed Res Int* **2013**, *2013*, 821498, <https://doi.org/10.1155/2013/821498>.
46. Lai, H.S.; Chen, W.J.; Chiang, L.Y. Free radical scavenging activity of fulleranol on the ischemia-reperfusion intestine in dogs. *World J Surg* **2000**, *24*, 450-4, <https://doi.org/10.1007/s002689910071>.

47. Mason, R.B.; Pluta, R.M.; Walbridge, S.; Wink, D.A.; Oldfield, E.H.; Boock, R.J. Production of reactive oxygen species after reperfusion in vitro and in vivo: protective effect of nitric oxide. *J Neurosurg* **2000**, *93*, 99-107, <https://doi.org/10.3171/jns.2000.93.1.0099>.
48. Fluri, F.; Grünstein, D.; Cam, E.; Ungethuen, U.; Hatz, F.; Schäfer, J.; Samnick, S.; Israel, I.; Kleinschnitz, C.; Orts-Gil, G.; Moch, H.; Zeis, T.; Schaeren-Wiemers, N.; Seeberger, P. Fullerenols and glucosamine fullerenes reduce infarct volume and cerebral inflammation after ischemic stroke in normotensive and hypertensive rats. *Exp Neurol* **2015**, *265*, 142-51, <https://doi.org/10.1016/j.expneurol.2015.01.005>.
49. Jeong, J.J.; Ha, Y.M.; Jin, Y.C.; Lee, E.J.; Kim, J.S.; Kim, H.J.; Seo, H.G.; Lee, J.H.; Kang, S.S.; Kim, Y.S.; Chang, K.C. Rutin from *Lonicera japonica* inhibits myocardial ischemia/reperfusion-induced apoptosis in vivo and protects H9c2 cells against hydrogen peroxide-mediated injury via ERK1/2 and PI3K/Akt signals in vitro. *Food Chem Toxicol* **2009**, *47*, 1569-76, <https://doi.org/10.1016/j.fct.2009.03.044>.
50. Schwarz, K.B. Oxidative stress during viral infection: a review. *Free Radic Biol Med* **1996**, *21*, 641-9, [https://doi.org/10.1016/0891-5849\(96\)00131-1](https://doi.org/10.1016/0891-5849(96)00131-1).
51. Di Carlo, M.; Giacomazza, D.; Picone, P.; Nuzzo, D.; San Biagio, P.L. Are oxidative stress and mitochondrial dysfunction the key players in the neurodegenerative diseases? *Free Radic Res* **2012**, *46*, 1327-38, <https://doi.org/10.3109/10715762.2012.714466>.
52. Lin, M.T.; Beal, M.F. Mitochondrial dysfunction and oxidative stress in neurodegenerative diseases. *Nature* **2006**, *443*, 787-95, <https://doi.org/10.1038/nature05292>.
53. Robea, M.-A.; Savuca, A.; Strungaru, S.A.; Lenzi, C.; Grasso, C.; Plavan, G.; Ciobica, A.; Nicoara, M. The general biological relevance of the oxidative stress status in replicating some neuropsychiatric and digestive-related manifestations in zebrafish. *Rom Biotechnol Lett* **2019**, *24*, 571-9, <https://doi.org/10.25083/rbl/24.4/571.579>.
54. Reuter, S.; Gupta, S.C.; Chaturvedi, M.M.; Aggarwal, B.B. Oxidative stress, inflammation, and cancer: how are they linked? *Free Radic Biol Med* **2010**, *49*, 1603-16, <https://doi.org/10.1016/j.freeradbiomed.2010.09.006>.
55. Oancea, S.; Mila, L.; Ketney, O. Content of Phenolics, in vitro Antioxidant Activity and Cytoprotective Effects against Induced Haemolysis of Red Cabbage Extracts. *Rom Biotechnol Lett* **2019**, *24*, 1-9, <https://doi.org/10.25083/rbl/24.1/1.9>.
56. Rehman, S.S.; Ashraf, A.; Nazli, Z.; Kausar, A.; Rafique, N.; Perveen, S.; Majeed, H.N.; Shafiq, N. Anticancer Activity of Natural Bioactive Compounds against Human Carcinoma Cell Lines-A mini review. *Rom Biotechnol Lett* **2019**, *24*, 937-44, <https://doi.org/10.25083/rbl/24.6/937.944>.
57. Trofin, F.; Ciobica, A.; Honceriu, C.; Cojocaru, S.I.; Stoica, B.; Cojocaru, D.; Ciornea, E.; Timofte, D. Modulatory effects of vitamin C on the relation between physical exercising and oxidative stress at young smokers. *Rom Biotechnol Lett* **2017**, *22*, 12439-47.
58. Jiang, B.; Liu, J.H.; Bao, Y.M.; An, L.J. Catalpol inhibits apoptosis in hydrogen peroxide-induced PC12 cells by preventing cytochrome c release and inactivating of caspase cascade. *Toxicol* **2004**, *43*, 53-9, <https://doi.org/10.1016/j.toxicol.2003.10.017>.
59. Luo, P.; Chen, T.; Zhao, Y.; Xu, H.; Huo, K.; Zhao, M.; Yang, Y.; Fei, Z. Protective effect of Homer 1a against hydrogen peroxide-induced oxidative stress in PC12 cells. *Free Radic Res* **2012**, *46*, 766-76, <https://doi.org/10.3109/10715762.2012.678340>.
60. Radu, B.M.; Osculati, A.M.M.; Suku, E.; Banciu, A.; Tsenov, G.; Merigo, F.; Di Chio, M.; Banciu, D.D.; Tognoli, C.; Kacer, P.; Giorgetti, A.; Radu, M.; Bertini, G.; Fabene, P.F. All muscarinic acetylcholine receptors (M(1)-M(5)) are expressed in murine brain microvascular endothelium. *Sci Rep* **2017**, *7*, 5083, <https://doi.org/10.1038/s41598-017-05384-z>.
61. Bernas, T.; Dobrucki, J. Mitochondrial and nonmitochondrial reduction of MTT: interaction of MTT with TMRE, JC-1, and NAO mitochondrial fluorescent probes. *Cytometry* **2002**, *47*, 236-42, <https://doi.org/10.1002/cyto.10080>.